2024 IEEE/RSJ International Conference on Intelligent Robots and Systems (IROS)
October 14-18, 2024. Abu Dhabi, UAE

SNU-Avatar Haptic Glove: Novel Modularized Haptic Glove via Trigonometric Series Elastic Actuators

Eunho Sung[1], Seungbin You[1], Seongkyeong Moon[1], Juhyun Kim[1] and Jaeheung Park[1,2]

***Abstract*— The avatar robot is a robot capable of realistic remote operation. In remote operation, the controllability of the glove is crucial. This glove can manipulate the hand interacting directly with the environment at the remote site. The glove must be able to accurately estimate the hand posture and provide haptic feedback to convey information about the remote environment and enhance operability. Throughout the process, user discomfort should be minimized. To achieve this goal, the research proposes providing force feedback to the fingers using Trigonometric Series Elastic Actuators. Haptic gloves are attached to the Middle Phalanx to facilitate the easy installation of additional add-ons, ensuring users feel securely fixed when attached. Additionally, by proposing an algorithm to estimate the fingertip position without directly attaching it to the fingertip, the haptic glove estimates hand posture and delivers appropriate force as needed. Finally, the system, including the haptic glove, participated in the ANA Avatar XPRIZE competition. The avatar system performed eight missions, which included not only remote manipulation of objects but also social interactions, demonstrating its effectiveness.**

I. INTRODUCTION

With the advancement of robot technology, one area of growing significance is teleoperation, exemplified by initiatives like the DARPA Robotics Challenge [1]. This competition tested the feasibility of employing robots instead of humans for tasks in disaster zones and hazardous environments, valve operations, and wall penetration. Subsequent to this, the 2021 ANA AVATAR Xprize challenge semi-finals explored the potential for remote robot usage in more nuanced activities like human interaction [2]. The global COVID-19 pandemic further underscored the importance of remote operations and communication, bringing increased attention to competitions like the ANA AVATAR Xprize. Notably, our research team, Team SNU (Seoul National University), excelled in the 2021 semifinals and progressed to the 2022 finals[3], [4]. In this study, the novel haptic glove developed by Team SNU for the finals is introduced, and its performance is demonstrated with experimental analysis.

*This work was supported by the National Research Foundation of Korea (NRF) grant funded by the Korea government (MSIT) (No. RS-2024-00461583). This work was also supported by the Technology Innovation Program (RS-2024-00423940) funded By the Ministry of Trade, Industry & Energy(MOTIE, Korea)

[1]Eunho Sung, Seungbin You, Seongkyeong Moon and Juhyun Kim are with the Department of Intelligence and Information, Graduate School of Convergence Science and Technology, Seoul National University, Seoul 08826, Republic of Korea. {eunho526, ysb0127, seongky.moon, ggdd1229}@snu.ac.kr

[2]Jaeheung Park is with the Department of Intelligence and Information, Graduate School of Convergence Science and Technology, ASRI, RICS, Seoul National University, Seoul 08826, Republic of Korea, and the Advanced Institutes and Advanced Institutes of Convergence Technology (AICT) Suwon 16229, Republic of Korea. park73@snu.ac.kr

Fig. 1: SNU-Avatar haptic glove is installed on the haptic device and is being operated by an operator.

To design an suitable glove for teleoperation tasks, two primary considerations must be addressed. Firstly, there is the need to accurately capture the kinematic position information of the fingers and send it to the robot hand. Secondly, it is essential to analyze methods for dynamically provide haptic feedback to the user for improving the user operability. The translation of human finger movements into commands for a robot hand is challenging due to the intricate structure of the human hand, which comprises 32 muscles and 27 degrees of freedom [5].

Researchers have explored various methods to effectively capture finger movement data. While the use of Inertial Measurement Unit (IMU) sensors is prevalent, it is limited by issues of reliability and stability [6], [7]. Lee et al. improved accuracy by combining IMU with vision sensors, whereas Chan et al. integrated flex bending sensors for enhanced precision [8], [9]. However, vision-based sensors are sensitive to light and require trackers, thereby imposing spatial constraints. An exoskeletal or soft glove approach also chosen, utilizing positional sensors to accurately and reliably determine the position information of the joints. The hard exoskeletal type provides robust force sensations and solid data tracking, as exemplified by Fang et al.'s comprehensive force feedback glove [10]. Nevertheless, its weight and complexity present maintenance challenges [11], [12]. Conversely, the soft wearable type, which employs tendon length positional sensors, such as Tran et al.'s silicon-based glove [13] and Tsabedze's TSA-driven glove [14], avoids hindering hand movements but encounters difficulties in individual fitting and actuator integration.

Secondly, gloves designed for teleoperation require a hap-

tic feedback mechanism to enhance task efficiency. Various methods have been proposed, including the use of oscillators to simulate the presence of force, exemplified by Estes et al.'s wearable vibration glove [15]. Other approaches, such as Okui et al.'s wearable air-jet device [16] and Qi et al.'s untethered pneumatic glove [17], stimulate sensation through the use of air jets or pneumatics. Constraints on glove movement, such as brakes, are also employed, as demonstrated by Blake's MR fluids clutch [18] and Wang et al.'s MR fluid brake connected to tendons [19]. Furthermore, direct actuation applies external force to fingers, with Takahashi utilizing soft tendons and Mcgibben muscles to mimic human hand movement [20]. When using a force feedback-enabled Haptic Glove, especially for the fingers, ensuring the safety of human hands is essential. One solution is the use of a Series Elastic Actuator (SEA), which measures external force by the deformation of an elastic member and expresses the desired force. SEA's mechanical compliance makes it human-friendly and suitable for glove development. Esmatloo et al. utilized SEA to create force feedback in tendon-driven gloves [21], while Refour et al. implemented SEA in a rigid exoskeleton glove with a 4-bar linkage [22].

Among the various teleoperation glove methods, the design for the ANA Xprize finals was based on the assumption of conducting operations in real remote environments. Opting for an exoskeletal type based on a rigid frame rather than a soft glove, the aim was not for comfort in daily life but for precise remote operations. To ensure the stability of actual robot tasks, a robust position sensor-based approach was chosen to capture the kinematic position information of fingers. For haptic feedback, the necessity of active force feedback rather than passive constraints or sensations was recognized, aiming to sense external disturbances or the weight of grasped objects. Therefore, tendon-driven actuation was employed.

Finally, for ensuring stable wearing during operation, the SEA method was devised, utilizing a triangular linkage-based SEA to implement stable force feedback without adding additional sensors. This paper primarily focuses on mechanical analysis, encompassing the design of Trigonometric SEA based on the linkage structure to assess the structural endurance against applied loads. Additionally, the paper includes a performance evaluation of the force feedback and positional accuracy of finger module of glove. When using a force feedback-enabled Haptic Glove, especially for the fingers, ensuring the stable wearing of human hands is essential. The subsequent sections of the paper are organized as follows: Section II provides an introduction to glove design with modularized finger. Section III discusses the design of the Trigonometric SEA working mechanism and fingertip estimation algorithm. Section IV describes the experimental analysis, and finally, Section V concludes the study.

II. Glove Design

The haptic glove is composed of four distinct finger posture measurement modules, each assigned to monitor the thumb, index finger, middle finger, and ring finger of the human hand. The glove is strategically positioned on the dorsal surface of the hand, enveloping it in a manner that facilitates seamless interaction. Utilizing an Arduino Mega, the device captures and records data, encompassing both finger force feedback and the precise angle of individual joints. Bidirectional communication with a personal computer is achieved through serial communication, allowing for a smooth exchange of information.

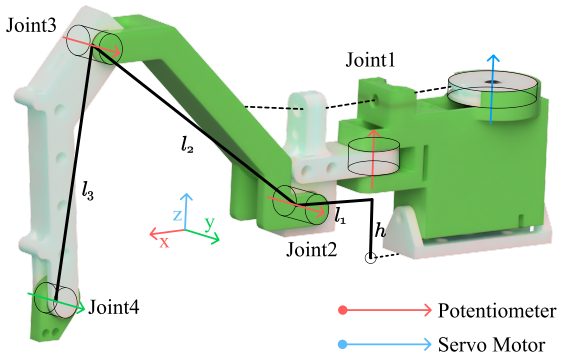

Fig. 2: SNU-Avatar haptic glove features a modular design for each finger, incorporating three potentiometers and one servo motor.

A. Modularized Finger

The finger module represents a pivotal component within the haptic glove, dedicated to the estimation of finger posture and the provision of force feedback. Each module is equipped with three potentiometers to gauge the finger's pose in space. It features a position control actuator and a spring for force feedback. The module's base includes a screw hole for integration with the haptic glove. The finger is securely fastened to the module using a flexible Velcro strap, ensuring an adaptable fit.

The finger module, designed to facilitate external power supply and data transmission, incorporates two types of terminals. The first terminal is constructed as a 5-pin terminal, with each pin incorporating three lines for the measurement of voltage, specifically Gnd, 5v, and three additional lines dedicated to the voltage measurement of three potentiometers. The second terminal comprises three pins for the servo motor.

The overall structure comprises 5 links and 4 joints. The first joint is specifically designed to measure the abduction-adduction (AA) movement of the MCP joint in the human finger using one of the three potentiometers. The second and third joints are engineered to assess the finger's pose resulting from the flexion-extension (FE) movement of the human finger joint, utilizing the remaining two potentiometers. Notably, in the case of second joint, it serves as the point where additional force feedback is applied.The potentiometer installed in this joint also determines the length of the actuator's tendon. The final joint is designed to alleviate potential discomfort, which arises from the changes in orientation between the links of the module and the human hand. This

joint does not feature any additional measuring device, with the primary objective of reducing friction through the use of a bearing.

Determining the position of the 4th joint is a key objective of the Modularized Finger. The specific configuration can be seen in Fig. 2. The position of the origin is where the floor intersects with the axis of joint 1. As seen in the Fig. 2, l1 measures 21.38mm, l_2 is $80mm$, l_2 is $65mm$, h is $29.8mm$. Using these lengths, the position of the 4th joint from the origin is given by Equation (1).

$$\begin{aligned} x_4 =& (l_2 \cos(\theta_{q_2}) + l_3 \cos(\theta_{q_2} + \theta_{q_3}) + l_1) \cos\theta_{q_1} \\ y_4 =& (l_2 \cos(\theta_{q_2}) + l_3 \cos(\theta_{q_2} + \theta_{q_3}) + l_1) \sin\theta_{q_1} \\ z_4 =& -l_2 \sin(\theta_{q_2}) - l_3 \sin(\theta_{q_2} + \theta_{q_3}) + h \end{aligned} \tag{1}$$

B. Glove Structure

The haptic glove introduced in the research exhibits a configuration where four modules, measuring the thumb, index finger, middle finger, and ring finger, are attached to a plate located on the dorsum of the hand as shown in Fig. 3. The overall size is represented as 250x175x130mm when unfolded, and when worn, it reaches a maximum length of 250mm to 340mm. The weight is approximately a 500 grams, encompassing the four modules, components in contact with the user's hand, Arduino board, and other elements.

The base frame of the glove plays a crucial role in integrating various internal and external components. Firstly, it connects to the finger modules. The joint between the glove base and finger modules is intentionally designed with high friction. This design accommodates the subtle variations in the orientation of the dorsum of the hand for each individual, occurring after the connection of the base frame and finger modules. As shown in Fig. 3, the haptic module is positioned considering the direction and location of the MCP joint of the SNU-Avatar Robot Hand [23]. This enabled hardware filtering, facilitating easier retargeting of high-degree-of-freedom fingers to the robot hand.

The second role involves integration with electronic components, including Arduino. an Arduino is located at the hypothenar of the palm, there is an Arduino for communicating with the computer. The Arduino is electrically connected to each module. Additional pins can be used to operate add-ons. In the competition, vibrators were installed on the fingertip and palm to establish additional interfaces. The third role is the connection between the human hand and the haptic glove. To accommodate various hand sizes and ensure a secure fit between the hand and the glove, the Boa System is employed. The Boa System assists in easily adjusting the tension of the string using ratchet gears. Additionally, the parts in contact with the hand are wraped with soft synthetic leather to enhance comfort during wear.

Lastly, there is a part that connected to the haptic arm. The respective parts are elongated pillar in shape and are located near the wrist. The attachment to the haptic arm is secure and utilizes a DovePlate, originally designed for coupling a camera and tripod.

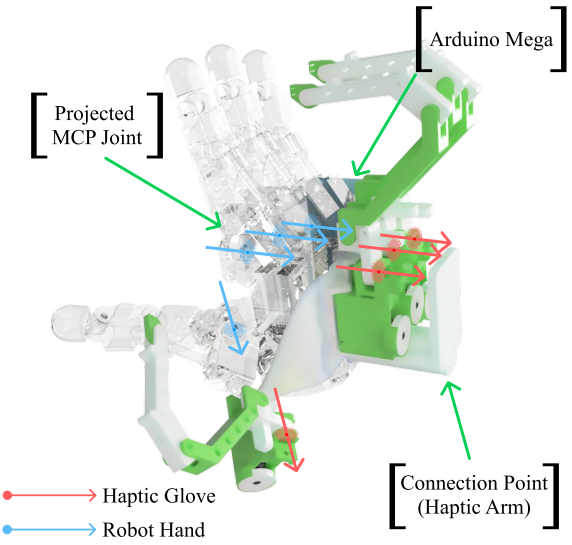

Fig. 3: The overall structure of the SNU-Avatar haptic glove is depicted, encompassing four modules referencing SNU-Avatar Robot hand [23], an Arduino Mega, and the connection point to the user's hand and the haptic arm.

III. Working Mechanism

The designed glove serves three primary roles. Firstly, glove involves estimating the posture of the fingers, which is crucial as it needs to manipulate the hand of a robot at a remote location. Secondly, glove generates a 1-degree-of-freedom movement using a single actuator for haptic feedback. Its operation is similar to Series Elastic Actuators (SEAs) in utilizing the change in length of an elastic element. The potentiometer located at joint2 is used to measure the deformation of the elastic element. Consequently, The use of a potentiometer located at joint2 for force feedback allows for a reduction in the number of encoders. Nonetheless, additional calculations are required to determine the deformation of the elastic element.

The third role of the haptic glove is the installation of a custom device for additional functionalities at the fingertip. To accommodate add-ons, space is needed at the fingertips. To secure this space, the haptic glove is coupled with the middle phalanxes of the user's fingers. Therefore, an algorithm is needed to estimate the position of the fingertip. This section explains additional calculation methods for force feedback and fingertip position estimation.

A. Trigonometric Series Elastic Actuators

The previously developed Series Elastic Actuators incorporate an elastic element between more than two encoders to generate force or torque. Trigonometric Series Elastic Actuators also requires two encoders. Among these, the encoder at the output side utilizes a potentiometer located slightly apart from the elastic material on joint2. The external encoder employs a trigonometric function for tendon length calculation. In Fig. 4, the tendon length is depicted as (2).

$$s = \sqrt{d^2 + l^2 - 2dl\cos\phi} \tag{2}$$

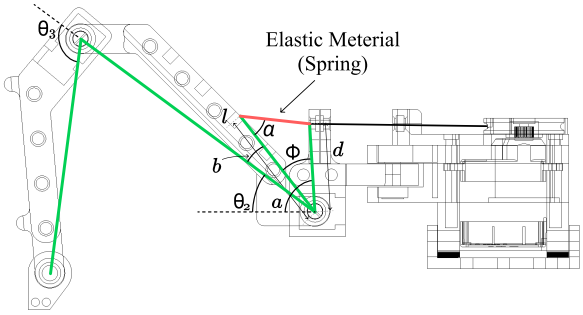

Fig. 4: The method of creating force feedback involves the servo motor pulling a cable, causing the spring to stretch as the cable shortens, generating resistance.

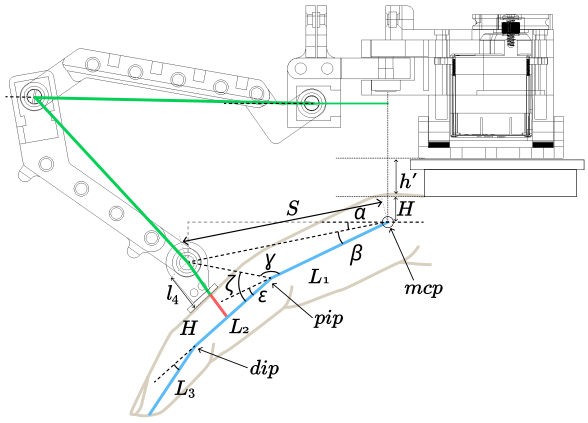

Fig. 5: The method of calculating the position of the finger's end effector utilizes the coupling between the dip joint and pip joint, estimating it based on the position of the middle phalanx.

When the user wears the haptic glove, changes in the angle of joint2 affect the spring. There are situations when force feedback is absent while using the remote control hand. The servo motor should operate in response to changes in joint2 while ensuring that no deformation occurs in the spring. The change in the angle of joint2 from ϕ_1 to ϕ_2 results in a corresponding alteration in tendon length. To control the tendon, the motor needs to move by an angle Δq. If we denote the radius of the pulley as r, the value of Δq can be expressed by the following Equation (3).

$$\Delta q = \frac{\left(\sqrt{d^2 + l^2 - 2dl\cos\phi_2} - \sqrt{d^2 + l^2 - 2dl\cos\phi_1}\right)}{r} \tag{3}$$

To generate force using Trigonometric Series Elastic Actuators, the pulley needs to re-tighten the tendon. If the motor winds an additional Δq_f, the force acting on the tendon can be calculated as Equation (4). Additionally, considering the initial position as θ_0 instead of θ_1 is possible for calculating the motor's angle. When the joint's angle is θ_0, the length of the tendon remains consistently at s_0.

$$F_s = k\left(\sqrt{d^2 + l^2 - 2dl\cos\phi_2} - s_0 - r\Delta q_f\right) \tag{4}$$

The force generated through Trigonometric Series Elastic Actuators is transmitted to the Middle Phalanx via the link3 of the module. Here, α can be expressed using the cosine law and the equation (2) derived from the calculation of the length of s, resulting in Equation (5). Taking Joint 2 as the origin, the torque equilibrium equation is expressed as Equation (6). Summarizing this for the force applied to the finger results in Equation (7).

$$\alpha = \arccos\left(\frac{l - d\cos\phi}{\sqrt{d^2 + l^2 - 2ld\cos\phi}}\right) \tag{5}$$

$$Fl_2\cos(\theta_3 - \pi/2) - F_s l\cos(\pi/2 - \alpha) = 0 \tag{6}$$

$$F = F_s\frac{l\sin\alpha}{l_2\sin\theta_3} \tag{7}$$

During the utilization of the glove, when the angle of Joint 2 is θ_2, and the desired force applied to the Middle Phalanx is denoted as F, the servo motor should have a q value as given in Equation (8) with $\Delta q = q - q_0$.

$$q = \frac{\left(\sqrt{d^2 + l^2 - 2dl\cos\phi_2} - s_0 - \frac{Fl_2\sin\theta_3}{kl\sin\alpha}\right)}{r} + q_0 \tag{8}$$

B. Estimation of Fingertip Position

Various techniques exist for mapping between a user-worn haptic device and a remote robotic hand. One approach involves estimating hand and finger poses using the haptic device and subsequently mapping them to a virtual hand model as demonstrated in our tested haptic glove or a robotic hand. Another method is to map directly using values without a virtual hand model [24]. In the proposed haptic glove discussed in this paper, the glove is affixed to the middle phalanx, restricting the direct determination of fingertip positions. To address this limitation, a finger model is employed, leveraging statistical information on human finger length ratios and the coupling between the DIP and PIP joints.

A human finger demonstrates four degrees of freedom in movement, characterized by four joints: MCP-adduction abduction, MCP - flexion extension, PIP, and DIP. The finger comprises four links, including a base link. Modeling the finger for position estimation involves utilizing assumptions drawn from previous research [25]. The initial assumption pertains to the relationship between the pip and dip joints.

$$\theta_{dip} = \frac{2}{3}\theta_{dip} \tag{9}$$

The second assumption pertains to the length ratios of the phalanges. This study presents statistical information on the length ratios of each finger's digits[26]. In the previous study, statistical information was presented regarding the length ratios of each digits. The current modeling assumes a length ratio of 0.50 - 0.30 - 0.20 for the proximal phalanx, middle phalanx, and distal phalanx, respectively. Utilizing the two

aforementioned assumptions, the finger can be modeled based on the angles of the two degrees of freedom in the MCP joint, the one degree of freedom in the PIP joint, finger length, total four variables. Assuming the position of the MCP joint is (0, 0, 0), the PIP joint, DIP joint, and end effector positions are as follows equation.

$$\begin{aligned} x_e =&(L_p \cos\left(\theta_{mcp_f}\right) + L_m \cos\left(\theta_{mcp_f} + \theta_{pip}\right) \\ &+ L_d \cos\left(\theta_{mcp_f} + \theta_{pip} + \theta_{dip}\right)) \cos\theta_{mcp_a} \\ y_e =&(L_p \cos\left(\theta_{mcp_f}\right) + L_m \cos\left(\theta_{mcp_f} + \theta_{pip}\right) \\ &+ L_d \cos\left(\theta_{mcp_f} + \theta_{pip} + \theta_{dip}\right)) \sin\theta_{mcp_a} \\ z_e =&L_p \cos\left(\theta_{mcp_f}\right) + L_m \cos\left(\theta_{mcp_f} + \theta_{pip}\right) \\ &+ L_d \cos\left(\theta_{mcp_f} + \theta_{pip} + \theta_{dip}\right) \end{aligned} \tag{10}$$

A haptic system consisting of two links becomes a unified system once attached to the user's middle phalanx. This system shares similarities with a 5-bar linkage system and a parallel SCARA robot arm. Utilizing these characteristics allows for the calculation of the posture up to the middle phalanx of the finger. Following, an algorithm is proposed to estimate the position of the finger end effector through the coupled movement of the finger's DIP and PIP joints

By employing models of the human finger and the Modularized Finger, the position of the 4th joint of the Modularized Finger can be determined from the human hand's MCP joint using two methods. One of these methods has been derived in Section II-A. Consequently, the calculation for the 4th joint position will be performed using the finger model. The intersection of the human finger and Modularized Finger occurs vertically at the middle phalanges of the human hand. Utilizing this information along with Equation (11), the distance to the 4th joint can be computed.

$$\begin{aligned} x_4 =&(L_p \cos\left(\theta_{mcp_f}\right) + (L_m/2) \cos\left(\theta_{mcp_f} + \theta_{pip}\right) \\ &+ (H + l_4) \sin\left(\theta_{mcp_f} + \theta_{pip}\right)) \cos\theta_{mcp_a} \\ y_4 =&(L_p \cos\left(\theta_{mcp_f}\right) + (L_m/2) \cos\left(\theta_{mcp_f} + \theta_{pip}\right) \\ &+ (H + l_4) \sin\left(\theta_{mcp_f} + \theta_{pip}\right)) \sin\theta_{mcp_a} \\ z_4 =&- L_p \sin\left(\theta_{mcp_f}\right) - (L_m/2) \sin\left(\theta_{mcp_f} + \theta_{pip}\right) \\ &+ (H + l_4) \sin\left(\theta_{mcp_f} + \theta_{pip}\right) \end{aligned} \tag{11}$$

In the previous equation, four values are required to determine the distance to the Modularized Finger's 4th joint. Two values are related to length, requiring knowledge of the finger's thickness and length. The remaining values require knowledge of the angles at the finger's MCP and PIP joints, influencing flexion-extension. To ascertain the finger's length and joint angle, three predefined hand postures will be used before wearing the glove.

One method involves stretching the hand, measuring the length from the finger's MCP joint to the middle phalanges. The estimated overall finger length is then derived from this measurement. The second method involves bending all fingers except the thumb. Using this posture and the previously measured finger length, the finger's thickness is calculated. The last posture is similar to the second, concentrating on bending only the thumb. This action is executed separately

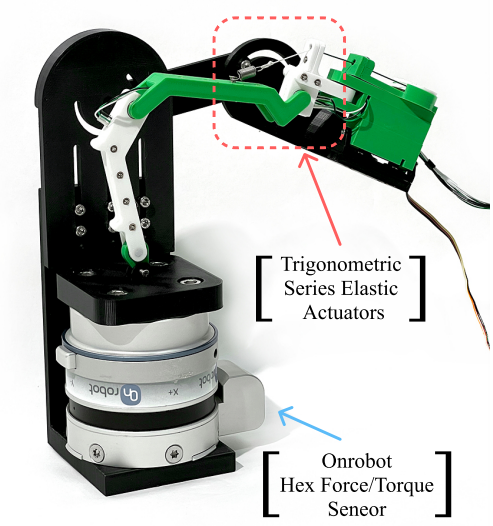

Fig. 6: The experimental setup for force feedback measurement involved the use of force torque sensors.

to prevent interference among the fingers. In the first posture, with all fingers extended, the relationship between the position of the Modularized Finger's 4th joint and L, h is as $x_1 = L_p + L_m/2 = 0.65L$. In the second posture, with the fingers bent, the relationship between the position of the fourth joint and L, h is as $z_2 = L_p + 2H$. The expressions for L and h are equivalent to Equation (12).

$$\begin{aligned} L =& x1/0.65 \\ H =& \left(z_2 - 6x_2/13\right)/2 \end{aligned} \tag{12}$$

In the previous Section II-A, the information that the distance to the fourth joint of this mechanism can be expressed as Equation (1), employing the Modularized Finger, is established. Employing the position of the 4th joint and the lengths L, H obtained through calibration, the angles of the MCP and PIP joints of the human finger can be calculated. The calculations, including the cosine law and trigonometric functions, can be performed with specific descriptions provided in the Appendix . Utilizing the assumed Equations (11) and Equations (12), the position of the fingertip can be calculated.

IV. Experimental Analysis

This section evaluates the suitability and performance of the proposed SNU-Avatar Haptic Glove for the avatar system. First, in Section III-A, an assessment is made regarding the force generated by the proposed Trigonometric SEA. Second, the performance of the algorithm proposed in Section III-B for estimating fingertip position is evaluated. Lastly, the Grasp taxonomy is evaluated with the SNU-avatar robot hand [23]. These experiments aim to confirm whether the SNU-avatar haptic glove can manipulate an actual robot hand.

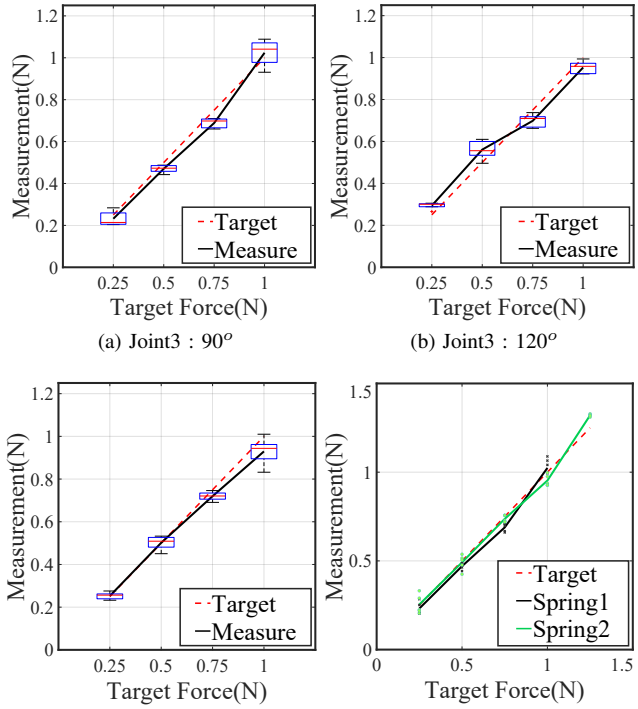

(a) Joint3 : 90^o (b) Joint3 : 120^o

(c) Joint3 : 135^o (d) Spring1 vs Spring2

Fig. 7: Results of the force feedback experiments. (a) corresponds to an angle of 90^o for Joint3, (b) to 120^o, and (c) to 135^o. In (d), the results are obtained using a spring with a higher elasticity coefficient compared to the original spring.

A. *Force feedback*

To evaluate the Trigonometric SEA, force measurements are conducted using a 6-axis force-torque sensor. The experimental setup is depicted in Fig. 6. The experiment was conducted using a single module. The part of the module connected to the finger was attached to the force-torque sensor. The part of the module connected to the human hand via the base was firmly fixed.

The experiment consisted of two main parts. In the first experiment, the angle of joint 3 of the module during the experiment. Four target forces were selected: 0.25N, 0.5N, 0.75N, and 1.0N. The experiment was repeated five times. In the second experiment, the experiment was conducted by changing the springs. Different elastic coefficients were used to test whether the four target forces could be achieved. Additionally, it was verified larger forces could be achieved using springs with higher elastic coefficients.

In Fig. 7, the plots correspond to the cases where the angle of joint 3 is 90 degrees, 120 degrees, and 135 degrees, respectively. The x-axis represents the target force, while the y-axis represents the measured values from the experiment. The red dashed line represents the ideal scenario. The closer the black solid line is to the red dashed line, the better the result.The maximum error observed in the data is 0.0704N, occurring when the angle of joint 3 is 135 degrees with a target force of 1.0N. The minimum error identified is

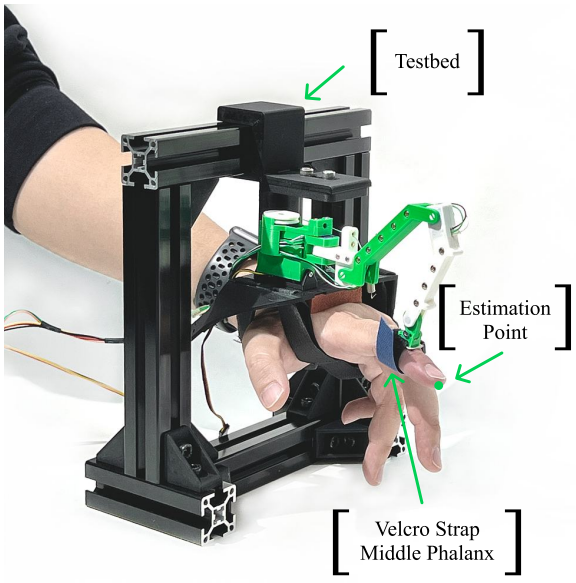

Fig. 8: The experimental setup for estimating the end effector position of the human finger involved securing the haptic glove on a testbed using an aluminum frame.

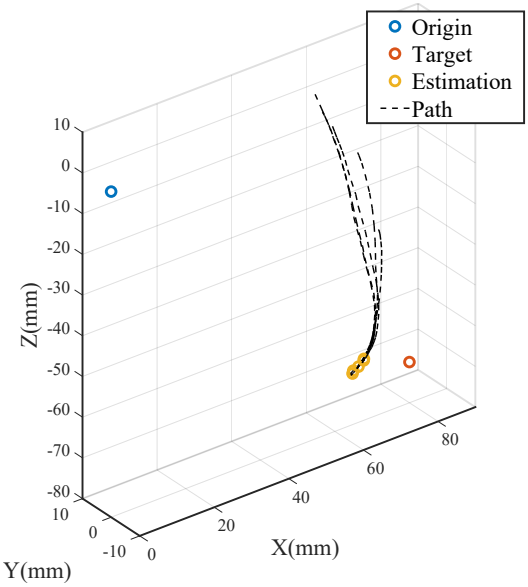

Fig. 9: The results of estimating the fingertip position with glove module

0.0016N, observed when the angle of joint 3 is 135 degrees with a target force of 0.5N.

For the second experiment, a spring with a higher elastic modulus was utilized. This was employed to generate greater force due to constraints in the structural space, limiting the deformation length of the spring. The elastic modulus was 1.2 times higher than the original value used. This adjustment was reflected in Equation 8. The results can be observed in Fig. 7(d), where the blue solid line represents the graph with the modified spring. It successfully achieves up to 1.25N. In this scenario, the error is 0.071N.

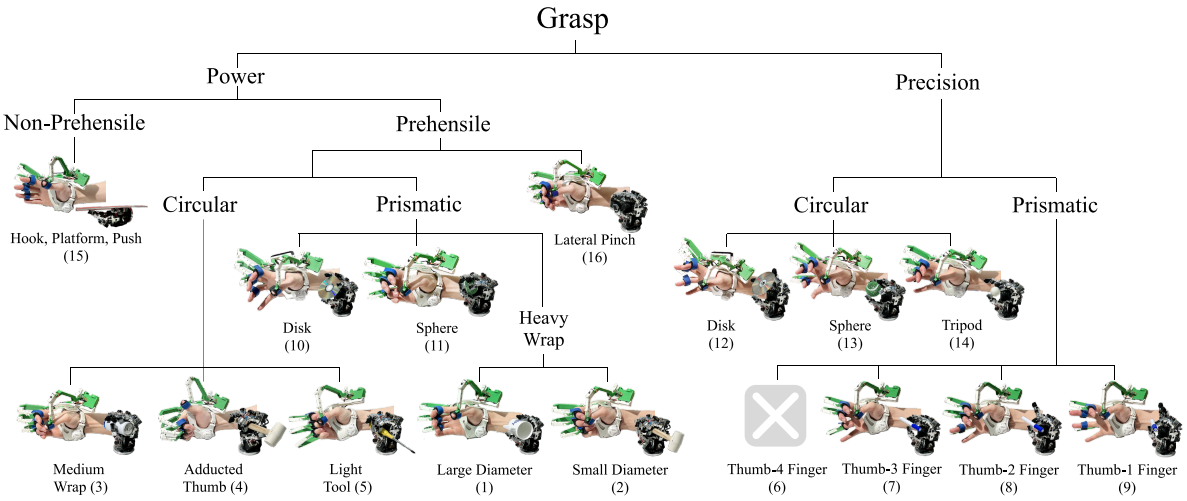

Fig. 10: Grasp taxonomy of the proposed SNU Avatar glove - SNU Avatar hand

B. Finger Position Estimation

To evaluate the effectiveness of fingertip position estimation for the role of the Haptic Glove, evaluation experiments were conducted. The experimental setup is depicted in Fig. 8. An additional apparatus was fabricated to immobilize the Haptic Glove attached to the hand, preventing its movement. Similar to the previous experiment, the evaluation was conducted for one module. The module was coupled to the Middle Phalanx of the human hand. The experiment entailed positioning a structure at the target point. The procedure encompassed making contact between the fingertip and the structure, repeated five times. This procedure was repeated five times.

The experimental results are plotted in Fig. 9, where each axis represents x, y, and z in millimeters. The blue dot represents the reference point at $(0, 0, 0)$. The red dot denotes the target point at $(80, 0, -70)$. The solid line illustrates the path taken to reach the target point. The yellow dot indicates the estimated fingertip position. It is evident that the data exhibits an overall biased result. The minimum error is 11.6mm, and the maximum error is 14.12mm. Specifically, there is an error of 13.9mm along the x-axis, 1.7mm along the y-axis, and 1.3mm along the z-axis. The repeatability precision is excellent, but the absolute error is considerable. There could be several reasons for this. Firstly, error could be attributed to the inaccuracy of the human hand model. We made two assumptions regarding the proportion of the phalanges and the relationship between the pip joint and dip joint. The second reason is the accuracy of the coupling between the human hand and the haptic glove. Accurately coupling and securing the human hand to the haptic glove is challenging. More data from additional individuals needs to be utilized. Additional structures should be implemented to allow the module to adjust its position along the x-axis of the base.

C. Grasping with the Tele-Operating Hand

To verify the compatibility of the Haptic Glove with the Robot Hand, we conducted a Grasp Taxonomy focusing on the hand's ability to perform missions effectively. The results are depicted in Fig. 10. We confirmed that the glove seamlessly implements the hand's movements, excluding category (6) which is structurally unfeasible for the hand. Based on these findings, we proceeded to perform missions in the ANA Avatar XPRIZE finals.

V. CONCLUSIONS

This study presents the design, fabrication, and analysis of the SNU-avatar Haptic Glove, developed for remote-operated robots. The glove was manufactured using a 3D printer and consists of three potentiometers and one servomotor to construct finger modules. We utilized a Trigonometric SEA to share one potentiometer, one of the duplicated components could be removed. The modules are attached to the middle phalanx, providing stable coupling, and allowing the possibility of installing additional add-ons on the fingertip. Despite being attached to the middle phalanx, fingertip position estimation is achievable through joint coupling of the fingers. Furthermore, we verified the effective movement of a remote robot hand through Grasp Taxonomy assessment. The proposed SNU-avatar Haptic Glove demonstrated excellent performance in the ANA Avatar XPRIZE finals. We plan to develop additional add-ons to provide sensations beyond haptic feedback, such as temperature, vibration, and touch. Moreover, we will implement re-take algorithms utilizing human hand synergy.

APPENDIX

The distance from the MCP joint to Joint 4 is denoted as S, and it is represented by Equation (13). Furthermore, the value of S_2 remains constant regardless of movement, as expressed in Equation (14). Moreover, the angle ζ in the same triangle can be calculated using Trigonometric functions, as shown in Equation (15).

$$S = \sqrt{x_4^2 + y_4^2 + (z_4 + H)^2} \tag{13}$$

$$S_2 = \sqrt{(L_m/2)^2 + (H + l_4)^2} \tag{14}$$

$$\zeta = \arctan \frac{H + l_4}{L_m/2} \tag{15}$$

Through this, beta can be calculated using the cosine rule in the triangle formed by the MCP joint, PIP joint, and the glove's joint 4, as expressed in Equation (17).

$$\alpha = \arctan \left(\frac{z_4 + H}{S} \right) \tag{16}$$

$$\beta = \arccos \left(\frac{S^2 + L_p^2 - (S_2)^2}{2SL_p} \right) \tag{17}$$

Secondly, leveraging the previously calculated values of s2', L, and the length of the proximal phalanx, gamma can be computed using the equation below. Using the calculated value of gamma and the previously determined ζ, ϵ can also be computed.

$$\gamma = \arccos \left(\frac{S_2^2 + L_p^2 - S^2}{2S_2L_p} \right) \tag{18}$$

$$\epsilon = \gamma + \zeta - \pi \tag{19}$$

The values of the MCP and PIP joints can be determined using the results above: MCP joint value is given by $\theta_{mcp} = \alpha + \beta$, and PIP joint value is given by $\theta_{pip} = \epsilon$.

REFERENCES

[1] S. Kim, M. Kim, J. Lee, S. Hwang, J. Chae, B. Park, H. Cho, J. Sim, J. Jung, H. Lee *et al.*, "Approach of team snu to the darpa robotics challenge finals," in *2015 IEEE-RAS 15th International Conference on Humanoid Robots (Humanoids)*. IEEE, 2015, pp. 777–784.

[2] K. Hauser, E. N. Watson, J. Bae, J. Bankston, S. Behnke, B. Borgia, M. G. Catalano, S. Dafarra, J. B. van Erp, T. Ferris *et al.*, "Analysis and perspectives on the ana avatar xprize competition," *International Journal of Social Robotics*, pp. 1–32, 2024.

[3] B. Park, D. Kim, D. Lim, S. Park, J. Ahn, S. Kim, J. Shin, E. Sung, J. Sim, J. Kim *et al.*, "Intuitive and interactive robotic avatar system for tele-existence: Team snu in the ana avatar xprize finals," *International Journal of Social Robotics*, pp. 1–29, 2024.

[4] B. Park, J. Jung, J. Sim, S. Kim, J. Ahn, D. Lim, D. Kim, M. Kim, S. Park, E. Sung *et al.*, "Team snu's avatar system for teleoperation using humanoid robot: Ana avatar xprize competition," in *RSS 2022 Workshop on "Towards Robot Avatars: Perspectives on the ANA Avatar XPRIZE Competition*, 2022.

[5] A. D. Deshpande, Z. Xu, M. J. V. Weghe, B. H. Brown, J. Ko, L. Y. Chang, D. D. Wilkinson, S. M. Bidic, and Y. Matsuoka, "Mechanisms of the anatomically correct testbed hand," *IEEE/ASME Transactions on mechatronics*, vol. 18, no. 1, pp. 238–250, 2011.

[6] J. Y. Oh, J. Lee, J. H. Lee, and J. H. Park, "Anywheretouch: Finger tracking method on arbitrary surface using nailed-mounted imu for mobile hmd," in *HCI International 2017–Posters' Extended Abstracts: 19th International Conference, HCI International 2017, Vancouver, BC, Canada, July 9–14, 2017, Proceedings, Part I 19*. Springer, 2017, pp. 185–191.

[7] Z. Yang, B.-J. F. Van Beijnum, B. Li, S. Yan, and P. H. Veltink, "Estimation of relative hand-finger orientation using a small imu configuration," *Sensors*, vol. 20, no. 14, p. 4008, 2020.

[8] Y. Lee, W. Do, H. Yoon, J. Heo, W. Lee, and D. Lee, "Visual-inertial hand motion tracking with robustness against occlusion, interference, and contact," *Science Robotics*, vol. 6, no. 58, p. eabe1315, 2021.

[9] T. K. Chan, Y. K. Yu, H. C. Kam, and K. H. Wong, "Robust hand gesture input using computer vision, inertial measurement unit (imu) and flex sensors," in *2018 IEEE International Conference on Mechatronics, Robotics and Automation (ICMRA)*. IEEE, 2018, pp. 95–99.

[10] H. Fang, Z. Xie, H. Liu, T. Lan, and J. Xia, "An exoskeleton force feedback master finger distinguishing contact and non-contact mode," in *2009 IEEE/ASME International Conference on Advanced Intelligent Mechatronics*. IEEE, 2009, pp. 1059–1064.

[11] E. Refour, B. Sebastian, and P. Ben-Tzvi, "Two-digit robotic exoskeleton glove mechanism: Design and integration," *Journal of Mechanisms and Robotics*, vol. 10, no. 2, p. 025002, 2018.

[12] R. E. Trott, T. J. Kleinig, S. L. Hillier, D. A. Hobbs, and K. J. Reynolds, "A modular hybrid exoskeletal-soft glove for high degree of freedom monitoring capability," in *2019 IEEE 16th International Conference on Rehabilitation Robotics (ICORR)*. IEEE, 2019, pp. 577–582.

[13] P. Tran, S. Jeong, F. Lyu, K. Herrin, S. Bhatia, D. Elliott, S. Kozin, and J. P. Desai, "Flexotendon glove-iii: Voice-controlled soft robotic hand exoskeleton with novel fabrication method and admittance grasping control," *IEEE/ASME Transactions on Mechatronics*, vol. 27, no. 5, pp. 3920–3931, 2022.

[14] T. Tsabedze, J. Trinh, A. Alomran, J. Clayton, and J. Zhang, "Design and characterization of award: An active wearable assistive and resistive device," in *2022 IEEE/ASME International Conference on Advanced Intelligent Mechatronics (AIM)*. IEEE, 2022, pp. 844–849.

[15] L. T. Estes, D. Backus, and T. Starner, "A wearable vibration glove for improving hand sensation in persons with spinal cord injury using passive haptic rehabilitation," in *2015 9th International Conference on Pervasive Computing Technologies for Healthcare (PervasiveHealth)*. IEEE, 2015, pp. 37–44.

[16] M. Okui, T. Masuda, T. Tamura, Y. Onozuka, and T. Nakamura, "Wearable air-jet force feedback device without exoskeletal structure and its application to elastic ball rendering," in *2020 IEEE/ASME International Conference on Advanced Intelligent Mechatronics (AIM)*. IEEE, 2020, pp. 276–281.

[17] J. Qi, F. Gao, G. Sun, J. C. Yeo, and C. T. Lim, "Hapt-glove—untethered pneumatic glove for multimode haptic feedback in reality–virtuality continuum," *Advanced Science*, vol. 10, no. 25, p. 2301044, 2023.

[18] J. Blake and H. B. Gurocak, "Haptic glove with mr brakes for virtual reality," *IEEE/ASME Transactions On Mechatronics*, vol. 14, no. 5, pp. 606–615, 2009.

[19] D. Wang, Y. Wang, J. Pang, Z. Wang, and B. Zi, "Development and control of an mr brake-based passive force feedback data glove," *IEEE Access*, vol. 7, pp. 172 477–172 488, 2019.

[20] N. Takahashi, S. Furuya, and H. Koike, "Soft exoskeleton glove with human anatomical architecture: production of dexterous finger movements and skillful piano performance," *IEEE Transactions on Haptics*, vol. 13, no. 4, pp. 679–690, 2020.

[21] P. Esmatloo and A. D. Deshpande, "Fingertip position and force control for dexterous manipulation through model-based control of hand-exoskeleton-environment," in *2020 IEEE/ASME International Conference on Advanced Intelligent Mechatronics (AIM)*. IEEE, 2020, pp. 994–1001.

[22] E. M. Refour, B. Sebastian, R. J. Chauhan, and P. Ben-Tzvi, "A general purpose robotic hand exoskeleton with series elastic actuation," *Journal of mechanisms and robotics*, vol. 11, no. 6, p. 060902, 2019.

[23] E. Sung, S. You, S. Kim, and J. Park, "Snu-avatar robot hand: Dexterous robot hand with prismatic four-bar linkage for versatile daily applications," in *2023 IEEE-RAS 22nd International Conference on Humanoid Robots (Humanoids)*. IEEE, 2023, pp. 1–8.

[24] S. Kim, E. Sung, and J. Park, "3-finger robotic hand and hand posture mapping algorithm for avatar robot," *Journal of Korea Robotics Society*, vol. 17, no. 3, pp. 322–333, 2022.

[25] C.-S. Chua, H. Guan, and Y.-K. Ho, "Model-based 3d hand posture estimation from a single 2d image," *Image and Vision computing*, vol. 20, no. 3, pp. 191–202, 2002.

[26] T. Ozsoy, Z. Oner, and S. Oner, "An attempt to gender determine with phalanx length and the ratio of phalanxes to whole phalanx length in direct hand radiography," *Medicine*, vol. 8, no. 3, pp. 692–7, 2019.